[CANCER RESEARCH 62, 4767–4772, August 15, 2002]

Promotion of Tumor Growth by Murine Fibroblast Activation Protein, a Serine Protease, in an Animal Model[1]

Jonathan D. Cheng,[2] Roland L. Dunbrack, Jr., Matthildi Valianou, André Rogatko, R. Katherine Alpaugh, and Louis M. Weiner

Department of Medical Oncology, Fox Chase Cancer Center, Philadelphia, Pennsylvania 19111

ABSTRACT

Fibroblast activation protein (FAP) is a type II integral membrane glycoprotein belonging to the serine protease family. Human FAP is selectively expressed by tumor stromal fibroblasts in epithelial carcinomas, but not by epithelial carcinoma cells, normal fibroblasts, or other normal tissues. FAP has been shown to have both *in vitro* dipeptidyl peptidase and collagenase activity, but its biological function in the tumor microenvironment is unknown. The modeled structure of murine FAP consists of a short cytoplasmic tail, a single hydrophobic transmembrane region, and a large extracellular domain. A seven-bladed β-propeller domain is situated on top of the catalytic triad and may serve as a "gate" to selectively filter protein access to the catalytic site. HEK293 cells transfected to constitutively express murine FAP, when xenografted into *scid* mice, were 2–4 times more likely to develop s.c. tumors and showed a 10–40-fold enhancement of tumor growth compared with mock-transfected HEK293 cells. Rabbits immunized with recombinant murine FAP developed polyclonal anti-FAP antibodies that significantly inhibited murine FAP dipeptidyl peptidase activity *in vitro*. HT-29 xenografts treated with these inhibitory anti-FAP antisera exhibited attenuated growth compared with tumors treated with preimmunization rabbit antisera. These data demonstrate the ability of FAP to potentiate tumor growth in an animal model. Moreover, tumor growth is attenuated by antibodies that inhibit the proteolytic activity of FAP. These findings suggest a possible therapeutic role for functional inhibition of FAP activity.

INTRODUCTION

FAP[3] is a type II integral membrane glycoprotein belonging to the serine protease family. Murine *Fap* has been sequenced and cloned (1) from embryonic mouse fibroblasts. It consists of a 2285-bp sequence composed of 761 amino acids with a calculated molecular weight of 88,000. Similar functional homology and an 89% shared sequence identity are seen between murine and human FAP. Human and murine FAP have been shown to have DPP activity (1, 2). Thus, FAP can cleave NH_2-terminal dipeptides from polypeptides with penultimate L-prolines or L-alanines (3). Mutation of the putative catalytic serine residue abolishes the proteolytic activity of FAP (4).

The expression of human FAP is highly specific for tumor fibroblasts. FAP is heavily expressed on reactive stromal fibroblasts in >90% of human epithelial carcinomas including those of the breast, lung, colorectum, and ovary (5). Neural and lymphoid cells, as well as surrounding normal tissue, lack demonstrable FAP expression. Epithelial carcinoma cells are also FAP negative. However, the function of FAP in the tumor microenvironment is unknown. Based on the selective expression of FAP in tumor fibroblasts, we hypothesized that inhibition of FAP proteolytic activity attenuated the invasive capabilities of tumors, leading to attenuated tumor growth. The results reported herein describe a modeled structure of murine FAP, the enhanced tumor growth and tumorigenicity of cell lines overexpressing FAP, and the ability of rabbit polyclonal anti-FAP antisera to inhibit FAP proteolytic function and alter *in vivo* tumor growth kinetics. In addition, we describe two distinct animal models that may be informative in future studies to elucidate the contributions of FAP to tumor growth and invasion.

MATERIALS AND METHODS

Modeled Protein Structure of Murine FAP. Murine FAP-ECD was modeled using the crystal structure of prolyl oligopeptidase (6), Protein Data Bank entry 1qfm. PSI-BLAST (7) was used to search the nonredundant protein sequence database to construct a position-specific similarity matrix for the sequence of FAP. A sequence database of proteins in the Protein Data Bank using the position-specific matrix was searched, and a match was found with the sequence of prolyl oligopeptidase, giving an expectation value of 6×10^{-57} and a sequence identity of 12% over 663 amino acids of FAP (residues 99–761). This covered all seven blades of the propeller and the hydrolase domain. The alignment in the propeller domain was manually adjusted to align conserved motifs in WD repeat proteins in the turns between β-strands. This resulted in significant changes in the alignment. In the hydrolase domain, only small manual adjustments were made upon consideration of the known structure of prolyl oligopeptidase.

Production of Recombinant Murine FAP-ECD Protein. Murine FAP cDNA was obtained from primary mouse embryonic fibroblast cultures. Reverse transcription-PCR reactions were carried out using primary cultured fibroblasts from BALB/c day 14.5 mouse embryos using Oligotex mRNA purification system (Qiagen, Valencia, CA) and reverse transcriptase/platinum Taq mix (Invitrogen, Carlsbad, CA) according to the manufacturer's instructions. The primers 5′-GGGGGGCCATGGCCATGAAGACATGGCGAAAACT-3′ and 5′-GGGGGGGCGGCCGCGTCTGATAAAGAAAAGCATTG-3′ were designed to anneal to the 5′ and 3′ ends of the National Center for Biotechnology Information GenBank murine FAP sequence accession number Y10007. The positions of the restriction sites *Nco*I and *Not*I are *underlined*. Murine FAP cDNA was re-engineered by PCR to eliminate the intracellular and transmembrane domains (the first 75 bp) for production of an ECD-secreted protein. The FAP-ECD cDNA was constructed by PCR with a $(His)_6$ epitope tag at the 5′ end and a FLAG epitope tag at the 3′ end and cloned into the pSEC/Tag2 expression vector. FAP-ECD was expressed in a mammalian system using the HEK293 human embryonic kidney cell line. HEK293 cells were maintained in DMEM + 10% fetal bovine serum and transfected with FAP-ECD using the FuGENE transfectant reagent (Roche, Indianapolis, IN) according to the manufacturer's instructions. Antibiotic-resistant clones were selected with 200 μg/ml hygromycin B and analyzed for FAP-ECD expression by Western analysis using antibodies to the FLAG and His tags. FAP-ECD-producing clone D4 was expanded, and Integra-1000 flasks (Integra Biosciences, Ijamsville, MD) were used for upscale protein production. Supernatants were collected twice weekly, and FAP-ECD was purified over a nickel-nitrilotriacetic-agarose column (Qiagen) for elution with 250 mM imidazole in immobilized met affinity chromatography buffer.

DPP Assay. Recombinant murine FAP-ECD was assayed for DPP activity using Ala-Pro-AFC as a substrate (Bachem, King of Prussia, PA). Serial dilutions of FAP-ECD were mixed with a 10-fold volume of reaction buffer consisting of 100 mM NaCl and 100 mM Tris (pH 7.8). An equal volume of 0.5 mM Ala-Pro-AFC in reaction buffer was added and incubated for 1 h at 37°C. Release of free AFC was measured in a Cytofluor fluorometer (Labsystems,

Received 12/21/01; accepted 6/20/02.

The costs of publication of this article were defrayed in part by the payment of page charges. This article must therefore be hereby marked *advertisement* in accordance with 18 U.S.C. Section 1734 solely to indicate this fact.

[1] Supported by NIH Grants CA06927 and CA01728, the Frank Strick Foundation, the Bernard A. and Rebecca S. Bernard Foundation, and an appropriation from the Commonwealth of Pennsylvania.

[2] To whom requests for reprints should be addressed, at Department of Medical Oncology, Fox Chase Cancer Center, 7701 Burholme Avenue, Philadelphia, PA 19111. Phone: (215) 728-2450; Fax: (215) 728-3639; E-mail: j_cheng@fccc.edu.

[3] The abbreviations used are: FAP, fibroblast activation protein; DPP, dipeptidyl peptidase; ECD, extracellular domain; AFC, 7-amido-4-trifluoromethylcoumarin.

Helsinki, Finland) with 395 nm excitation and 490 nm emission to quantitatively measure DPP activity. 480 V excitation was used with a band pass of 8, measured for 60 s in a time trace to obtain mean emission values. Testing of antibody inhibition of DPP activity was performed by incubating 12 μg of the saturated ammonium sulfate-purified rabbit polyclonal antibody with 12 ng of FAP-ECD for 30 min at 37°C before the addition of the Ala-Pro-AFC substrate. Tests were performed in triplicate and assayed with the Cytofluor fluorometer.

FAP Immunization. Two female New Zealand White rabbits were immunized by s.c. administration of 250 μg FAP-ECD/dose. The initial immunization was emulsified in Complete Freund's Adjuvant, with boost injections given every 3 weeks in Incomplete Freund's Adjuvant for a total of five FAP-ECD immunizations (1,250 μg/rabbit). Rabbits were bled preimmunization and 7–10 days after each boost dose to screen by ELISA for serum antibody induction. ELISA was performed in 96-well plates coated with 200 ng/well FAP-ECD in 50 mM $NaHCO_3$ (pH 9.6) coating buffer. After a 2-h incubation, the plates were washed and blocked with 1% BSA/Tween 20. The test bleed sera were diluted 1:50, and 50 μl/well were added for a 1.5-h incubation at room temperature. Secondary antibodies of goat antirabbit immunoglobulin were added in a 1:1,000 dilution. A tertiary antibody in a 1:10,000 dilution consisting of biotinylated rabbit antigoat IgG was then added, followed by horseradish peroxidase-streptavidin (1:10,000 dilution). 2,2′-azino-di-[3-ethylbenzthiazoline-6-sulfonic acid] (BroRad, Hercules, CA) substrate was added and analyzed at an absorbance of 405 nm with a 650 nm reference wavelength. All samples were performed in triplicate. Terminal bleeds were performed 14 weeks after immunization and yielded 100 ml sera/rabbit. The rabbit sera containing polyclonal antibodies were purified by ammonium sulfate precipitation (SAS cut). Saturated ammonium sulfate solution was slowly added to an equal volume of rabbit sera and precipitated overnight at 4°C. The mixture was centrifuged at 3,000 $\times$ *g* for 30 min at 4°C. The supernatant was discarded, and the pellet was resuspended in 15 ml of PBS (pH 7.2), dialyzed against PBS, and sterilely filtered using 0.2 μm syringe filter. SAS cut rabbit polyclonal antibodies were used for DPP inhibition assay, treatment of mice with HT-29 xenografts, and immunohistochemical staining of HT-29 and HEK-FAP tumors.

HEK-FAP Mouse Xenografts. HEK293 cells were chosen for study in an animal model because of their modest tumor growth rates and the ability of these cells to readily express transfected mammalian proteins. FAP cDNA was cloned into the pcDNA3 vector (Promega, Madison, WI) and transfected into HEK293 cells (American Type Culture Collection, Manassas, VA) using the FuGENE transfectant reagent (Roche) according to the manufacturer's instructions. Clones resistant to antibiotic selection by G418 (200 μg/ml) were selected and confirmed to express FAP by flow cytometry (data not shown). The negative control of HEK293 transfected with "empty" pcDNA3 vector was used for all experiments. Fifteen C.B17/Icr-*scid* mice received s.c. injection of 4×10^6 HEK293-FAP cells/mouse into their right flank and 4×10^6 HEK293-vector cells/mouse into their left flank, using each mouse as their own control. Similarly, 15 C.B17/Icr-*scid* mice received s.c. injection of 1×10^7 HEK293-FAP cells/mouse and 1×10^7 HEK293-vector cells/mouse into their right and left flanks, respectively. Animals were maintained in pathogen-free conditions in autoclaved microisolator cages in the Fox Chase Cancer Center Laboratory Animal Facility. Serial tumor measurements were obtained every 3–4 days by caliper in three dimensions. Tumor volumes were calculated by the following formula: volume = height $\times$ weight $\times$ length $\times$ 0.5236. Animals were followed until any mouse developed a tumor measuring 2 $\times$ 2 cm, was observed to be suffering, or appeared moribund. Animals were euthanized according to institutional policy.

Treatment of HT-29 Xenografts with Rabbit Anti-FAP Antibodies. National Institute for Health Cancer Research outbred nude mice bearing HT-29 (American Type Culture Collection) s.c. xenografts were used as an animal model because of the abundant FAP expression in the stroma of human colorectal carcinomas (8). Fifty ml of FAP-ECD-immunized rabbit sera or preimmunization sera were purified by ammonium sulfate precipitation. Cohorts of five nude mice were xenografted with 6×10^6 HT-29 cells/mouse and received i.p. injection of 1 mg/injection SAS cut FAP-immunized antibodies or preimmunization antibodies 3 times/week for 3 weeks. Serial tumor measurements were obtained 3 times/week by caliper in three dimensions, and volumes were calculated by the following formula: volume = height $\times$ weight $\times$ length $\times$ 0.5236. The experiment was terminated after tumors had grown for 21 days.

Immunohistochemistry. HEK-FAP or HT-29 tumors from C.B17/Icr-*scid* mice were snap-frozen in liquid nitrogen and stored at −70°C. Five-μm sections were cut and stained. Primary antibody of SAS cut rabbit polyclonal anti-FAP antisera was used in a 1:750 dilution (v/v). Amplification and development by BioGenex (San Ramon, CA) biotin-streptavidin detection system with horseradish peroxidase were performed as per the manufacturer's directions. The pattern of FAP expression in the tumor sections was assessed.

Statistical Analysis. Mixed model ANOVA was implemented to examine the effect of test (HEK293-FAP) *versus* control (HEK293-vector) on mouse tumor growth. The indicator variable identifying mice was included as a random classification factor to accommodate the repeated measures structure of the data. Toeplitz matrix was used to model the covariance structure. Standard diagnostic procedures were used to detect disagreement between the selected model and the data to which it is fitted. McNemar's test was applied to test the association between the matched pairs of test (HEK293-FAP) *versus* control (HEK293-vector) on mouse tumor growth coded as a binary variable (*e.g.,* presence or absence of tumor). To examine the effect of rabbit polyclonal sera treatment on HT-29 xenografts, repeated measures ANOVA was used to model the change of tumor size over time and compare FAP-immunized rabbit sera treatment *versus* preimmunization sera treatment controls in terms of temporal changes in tumor size. The correlation structure was modeled as first order autoregressive. Independent sample *t* test with Satterthwaite correction for unequal variances was used to compare treatment groups with respect to tumor size at each time point. Statistical analysis was performed using standard computer software statistical packages (SAS, MINITAB, StatXact). The critical significance level of 0.05 was chosen.

RESULTS

Modeled Structure of Murine FAP. The modeled structure (Fig. 1) of FAP consists of a short cytoplasmic tail (amino acids 1–6), a single hydrophobic transmembrane region (amino acids 7–25), and a large ECD (amino acids 26–761). The ECD is postulated to consist of two major domains, a seven-bladed β-propeller domain (amino acids 99–499) and an $\alpha\beta$ hydrolase domain (amino acids 500–761) that contains the catalytic triad. The catalytic triad consists of a serine at position 624, aspartic acid at position 702, and histidine at position 734. The triad is located in the central portion of FAP, with the seven-bladed β-propeller domain situated on top of the catalytic triad. This β-propeller domain provides sole access to the catalytic triad and may serve as a gate to selectively filter proteins down its cylindrical groove to the serine catalytic site.

Animal Models. Fig. 2 shows the distinctive FAP distribution patterns in two tumor models as demonstrated by immunohistochemistry. The FAP-transfected HEK293 xenografts (Fig. 2, *A* and *B*) express FAP on the cell surface as demonstrated by the surface membrane staining of the individual HEK293 cells. In contrast, FAP expression in HT-29 xenografts is seen in the intervening tumor stroma (Fig. 2, *C* and *D*), trabeculating between nests of HT-29 cells, as FAP staining is distinctly absent from the HT-29 cells themselves. Preimmunization rabbit sera showed no appreciable immunohistochemical staining over background (data not shown). The HEK293 xenografts demonstrate membrane surface expression of constitutively produced FAP, whereas the HT-29 tumors induce host stromal expression of FAP. The HT-29 xenograft FAP expression patterns are nearly identical to those seen clinically in human colorectal cancer (8). These two tumor models offer distinct FAP expression patterns and serve as useful *in vivo* models to test agents that modulate FAP biological activity. They were therefore used for further study assessing the immunomodulatory effects of FAP-specific antibodies.

FAP Potentiates Tumor Growth. Cohorts of 15 C.B17-*scid* mice each were inoculated with either 4×10^6 FAP-transfected HEK293 cells/mouse, 4×10^6 mock-transfected HEK293 cells/mouse, 1×10^7 FAP-transfected HEK293 cells/mouse, or 1×10^7

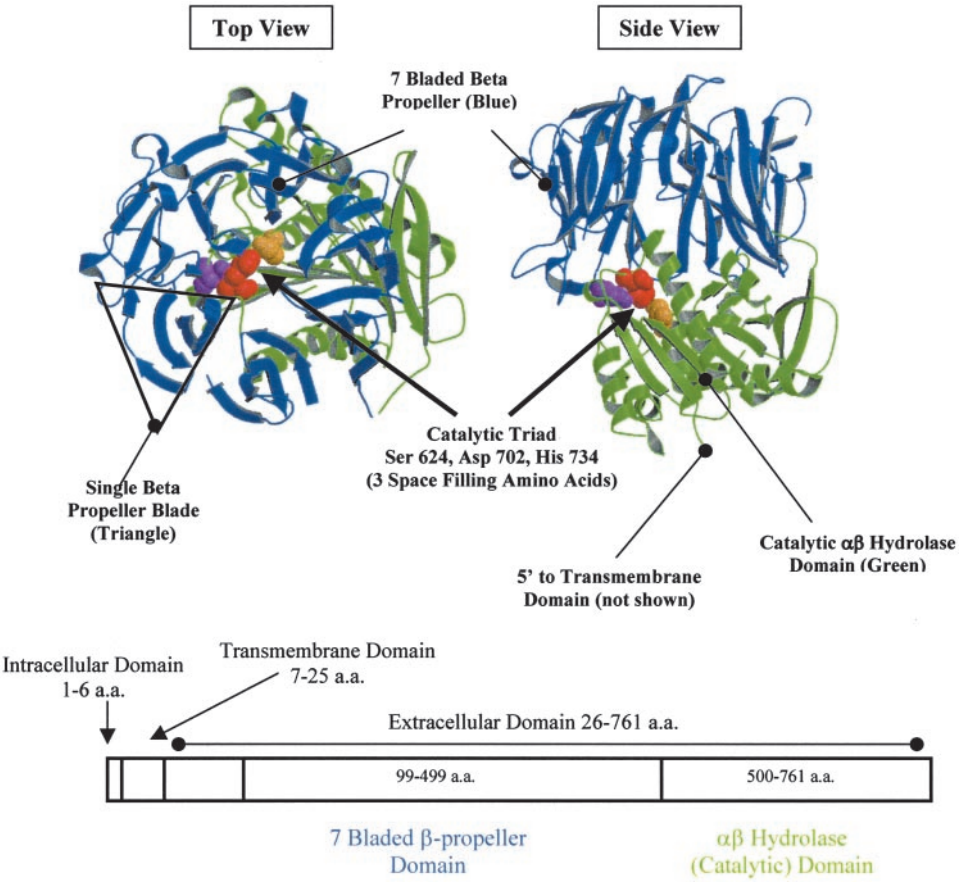

Fig. 1. Predicted murine FAP structure. The modeled structure shows FAP to have a short cytoplasmic tail (amino acids 1–6), a single hydrophobic transmembrane region (amino acids 7–25), and a large ECD (amino acids 26–761). The ECD consists of two domains, a seven-bladed β-propeller domain (amino acids 99–499) and an $\alpha\beta$ hydrolase domain (amino acids 500–761) that contains the catalytic triad. The catalytic triad consists of a serine at position 624, aspartic acid at position 702, and histidine at position 734.

mock-transfected HEK293 cells/mouse. Results are shown in Table 1. FAP-transfected HEK293 cells were 2–4 times more likely to develop tumors compared with mock-transfected HEK293 controls ($P = 0.0313$). The latency period, as measured from the day of inoculation until tumors were palpable, was shortened by 10–15 days by HEK-FAP tumors compared with HEK-mock tumor controls. A 10–40-fold enhancement in tumor growth was seen in mice inoculated with HEK-FAP cells compared with their corresponding mock-transfected controls ($P = 0.005$ for 4×10^6 cells/mouse, $P = 0.0001$ for 1×10^7 cells/mouse). The respective tumor growth curves are shown in Fig. 3. HEK293 cells transfected with FAP therefore demonstrated a greater propensity for tumor

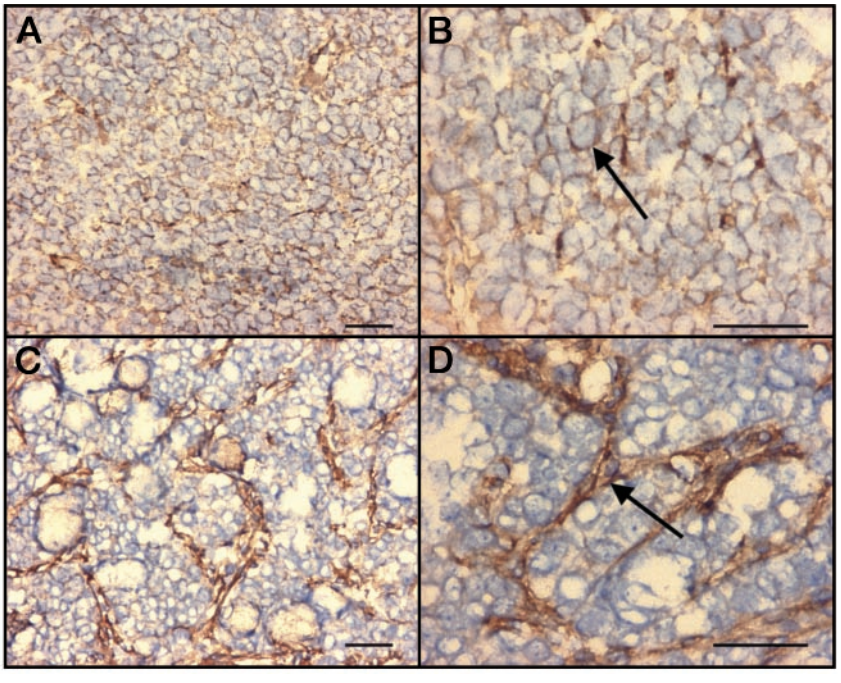

Fig. 2. Distinctive FAP expression in two animal tumor models. *A* and *B* represent immunohistochemical staining for FAP at ×20 and ×40 magnification, respectively, of FAP-transfected HEK293 cells revealing HEK293 cell membrane staining (*arrow*). *C* and *D* represent the same magnification demonstrating FAP expression in the stromal compartment of an HT-29 xenograft. The *arrow* identifies staining of the stromal fibroblasts, whereas tumor cells are negative for FAP expression. Staining was performed with a 1:750 dilution of rabbit polyclonal FAP antisera (see "Materials and Methods"). *Bar*, 50 μm.

Table 1 *Tumor growth of HEK293 xenografts*

Four cohorts of 15 mice each were inoculated with either 4×10^6 FAP-transfected HEK293 cells/mouse, 4×10^6 mock-transfected HEK293 cells/mouse, 1×10^7 FAP-transfected HEK293 cells/mouse, or 1×10^7 mock-transfected HEK293 cells/mouse. Mock transfection consisted of the negative control of HEK293 cells transfected with empty pcDNA3 vector. HEK293 cells transfected with FAP demonstrate a greater propensity for tumor development, a shortened latency period, and an enhanced growth rate compared with mock-transfected controls.

Cohort (15 mice/cohort)	Cells	No. of inoculated cells/mouse	No. of mice developing tumor	Tumor volume[a] (mean ± SE)	Days to palpable tumors[b] (mean ± SD)
1	HEK-FAP	4×10^6	8/15	498.4 ± 182.4	23.2 ± 8.1
2	HEK-Mock	4×10^6	2/15[c]	49.1[c] ± 49.1	33 ± 2.8
3	HEK-FAP	1×10^7	13/15	898.6 ± 151.4	9 ± 5.9
4	HEK-Mock	1×10^7	7/15[c]	21.8[c] ± 9.0	34 ± 3.6

[a] Mean tumor volume of all mice measured on the day mice were culled. Mice were culled on day 42 for cohorts 1 and 2 and on day 38 for cohorts 3 and 4.
[b] Mean days from inoculation until tumor first palpable in mice developing tumors.
[c] $P < 0.05$ comparing cohorts 1 and 2 or cohorts 3 and 4.

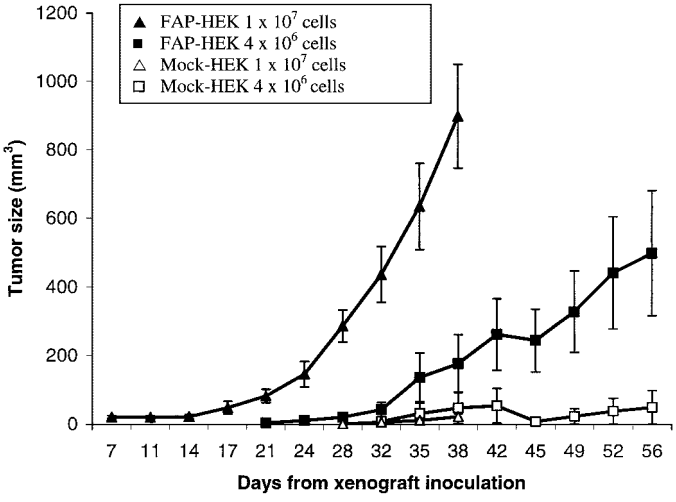

Fig. 3. Potentiation of tumor growth by FAP-transfected 293 cells. Tumor xenograft growth curves with SE bars of FAP-transfected HEK293 cells (▲ and ■) compared with mock transfection of HEK293 with empty vector (△ and □). Fifteen mice/cohort were xenografted with 1×10^7 FAP-transfected HEK293 cells/mouse (▲), 4×10^6 FAP-transfected HEK293 cells/mouse (■), 1×10^7 mock-transfected HEK293 cells/mouse (△), or 4×10^6 mock-transfected HEK293 cells/mouse (□). The top growth curves (▲ and ■) show the enhanced growth potential of FAP-transfected HEK293 cells compared with the negative control (△ and □) of empty vector-transfected HEK293 cells. $P = 0.0001$ for 1×10^7 cells/mouse (▲ *versus* △), and $P = 0.005$ for 4×10^6 cells/mouse (■ *versus* □).

Table 2 *Immunization of rabbits and mice with FAP-ECD*

Table 1 shows the absorbance at 405 nm of ELISA assays from serial time points of a representative rabbit immunized with FAP-ECD. Immunization led to a near 5-fold increased absorbance over baseline (column 3), demonstrating the successful production of anti-FAP antibodies.

Rabbit 26	Mean absorbance	Increase over baseline (fold)
Preimmunization	0.136	1.0
7 weeks after immunization	0.637	4.7
10 weeks	0.654	4.8
13 weeks	0.618	4.5

development, a shortened latency period, and an enhanced growth rate compared with mock-transfected controls.

Rabbit Polyclonal Anti-FAP Antibodies Inhibit DPP Activity and HT-29 Tumor Growth. FAP-immunized rabbit polyclonal antisera demonstrating FAP-ECD specificity (Table 2) were studied for modulation of FAP DPP activity using a fluorogenic DPP assay. Fig. 4 shows that the DPP activity of FAP is partially inhibited when the protein is preincubated with immunized rabbit sera. Fig. 5 shows moderate tumor growth attenuation of HT-29 xenografts in mice treated with rabbit polyclonal FAP antibodies compared with preimmunization control antibodies. This establishes the proof of principle that the proteolytic activity of FAP can be immunomodulated and may serve as a useful target for immunotherapeutics designed to alter FAP-induced tumor growth.

DISCUSSION

Although FAP expression in the tumor microenvironment has been well described (4, 5), its potential role in promoting tumor growth and metastasis has not been investigated previously. This work provides the first direct demonstration that overexpression of FAP confers an

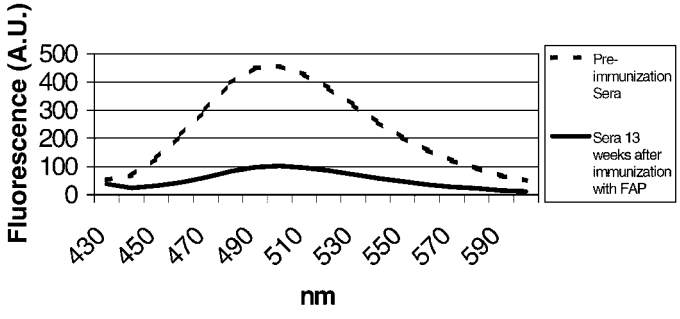

Fig. 4. Inhibition of DPP activity by FAP-specific rabbit polyclonal sera. Fluorescent emission spectrum measuring the release of free AFC from the Ala-Pro-AFC substrate by incubation with FAP-ECD is shown. The *dashed line* shows the DPP activity of FAP with preimmunization serum (mean absorbance = 0.136 by ELISA against FAP-ECD). The *solid line* shows the inhibition of FAP activity with serum from the same rabbit after 13 weeks of FAP immunization (mean absorbance = 0.618 by ELISA against FAP-ECD). This suggests that an appropriate antibody targeting FAP has the potential to inhibit the DPP activity of FAP.

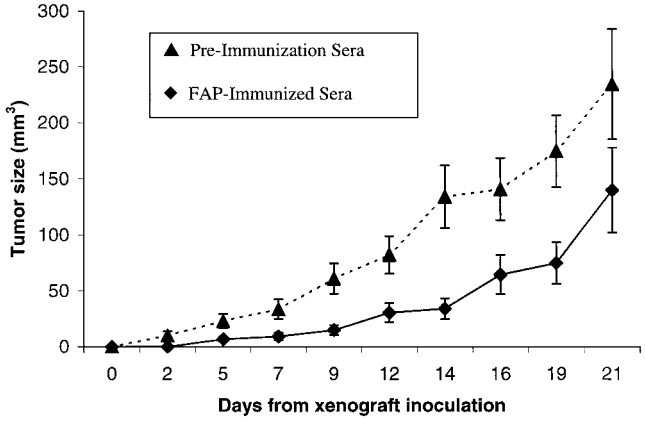

Fig. 5. Inhibition of tumor growth by FAP inhibitory antibodies. Two cohorts of five nude mice were xenografted with HT-29 colorectal carcinoma cells and injected i.p. 3 times/week for 21 days with 1 mg/injection SAS cut FAP immunized rabbit antibodies or preimmunization antibodies. Serial tumor measurements were obtained, demonstrating tumor growth inhibition of mice treated with rabbit polyclonal antibodies that have DPP inhibitory effects (Fig. 4), compared with preimmunization antibody controls. Tumor growth was found to be significantly different between the treatment and control cohorts for days 9–19 ($P = 0.0118$ for the two curves).

advantage for tumor growth (Fig. 3). Fibroblasts are known to have potent synergistic effects on *in vivo* and *in vitro* tumor formation and growth (9, 10). Fibroblasts coinoculated with carcinomas in mice have resulted in markedly shortened latency period (11) and enhanced tumor growth (12). Although these reports used whole fibroblast cells, they are consistent with our findings evaluating the effects FAP, a tumor stromal fibroblast protein. FAP exhibits a tightly controlled expression pattern, as it is not detectable by immunohistochemistry on normal fibroblasts or epithelial carcinoma cells (2, 8). This contrasts sharply to other tumor fibroblast-associated proteases such as matrix metalloproteinases or urokinase, which are far more ubiquitous in their expression patterns (13–18). The biological basis of the tightly regulated expression of FAP in the tumor microenvironment holds potential significance for understanding and interfering with tumor stromal biology. We demonstrate a novel tumor-stromal interaction mediated by FAP by which the host microenvironment modulates tumor growth properties.

This study lends insight into FAP biological function by demonstrating that FAP overexpression enhances tumorigenic potential and tumor growth rates in an animal model. As shown in Fig. 3, FAP-transfected HEK293 cells demonstrate a 2–4-fold greater tumorigenic potential, a shortened tumor latency period, and a 10–40-fold enhanced growth rate compared with mock transfected HEK293 cells. In addition, rabbit polyclonal antibodies that inhibit FAP catalytic activity can attenuate tumor growth in a colorectal cancer xenograft model. This observation lends weight to the growing body of evidence that factors in the tumor microenvironment provide critical frameworks for tumor growth and metastasis. Our animal model suggests that FAP may be an important component of this framework and an attractive therapeutic target.

The mechanism by which FAP enhances tumorigenicity and tumor growth in HEK293 cells is unclear. The enhanced tumor growth seen by transfection of HEK293 with FAP does not necessarily indicate oncogenic transformation because unmodified HEK293 cells exhibit moderate tumorigenic potential due to their cellular transformation by human adenovirus type 5 (19). The majority of mice xenografted with 4×10^6 unmodified HEK293 cells developed palpable tumors over the course of 3 months (data not shown). FAP transfection reduces the number of inoculated cells required to develop tumors, shortens the latency period until tumors become palpable, and enhances tumor growth rates. We speculate that FAP in fact does not lead to oncogenic transformation because in the HT-29 xenograft tumor model presented here, normal fibroblasts rather than colorectal cancer cells express FAP, yet these host fibroblasts do not form mesenchymal tumors.

Other serine proteases have demonstrated roles in tumor growth (20). For example, there is a strong correlation between urokinase plasminogen activator levels, poor prognosis, and greater metastatic potential in breast cancer (13). A distinctive feature that may lend insight into potential mechanisms of FAP-mediated tumor growth is that FAP is transiently expressed in normal wound healing (5). Tumors are able to maintain wound healing events through the expression of permeability factors, procoagulants, and chemotactic and mitogenic factors. It is appealing to conjecture that tumors subvert the role of FAP in normal wound healing to activate by its DPP enzymatic properties as yet undefined factors contributing to tumor growth. Further understanding of FAP biology may lend additional mechanistic insights into the concept that tumors are wounds that do not heal (21). Accordingly, the disruption of FAP function in tumors may represent a novel therapeutic strategy for interfering with tumor recruitment of stromally derived proteases, growth factors, or angiogenic or adhesion molecules.

Given that FAP has both dipeptidyl and collagenase activity, we hypothesized that the catalytic site of FAP would be a potential therapeutic target. Antibodies were developed with the goal of blocking FAP catalytic activity. Murine monoclonal antibodies produced through hybridoma methodology were found to have specificity for FAP but did not inhibit FAP enzymatic activity as measured in the DPP fluorescence assay (data not shown). However, rabbit sera containing FAP polyclonal antibodies were able to inhibit FAP activity as well as moderately attenuate tumor growth. The modest growth attenuation is consistent with our hypothesis that FAP catalytic activity is critical for its biological effect. We found that incomplete inhibition of FAP catalytic activity as seen *in vitro* (Fig. 4) led to moderate but incomplete *in vivo* growth inhibition as seen in Fig. 5. Although the effect of FAP inhibitory polyclonal antibodies *in vivo* is modest, these findings further establish the proof of principle that tumor-stromal interactions using FAP play an important role in tumor growth and invasion. Current efforts are aimed at developing more effective inhibitory antibodies to test in the animal models described here.

The antibodies specific for FAP have proven to be valuable probes to initiate the biological investigation of FAP. Rabbit polyclonal antisera were used to immunohistochemically stain the tumors in our animal models to examine the expression patterns of FAP. Two distinct patterns emerged (Fig. 2). The HEK-FAP-transfected xenografts demonstrated intense surface membrane staining encircling the individual HEK-FAP cells. In contrast, the HT-29 human colon cancer xenografts did not demonstrate staining of the colorectal cancer cells themselves, but strong FAP expression was detected in the stromal compartment and trabecular spaces between nests of HT-29 cells. This stromal expression pattern is identical to the expression pattern seen clinically in human colorectal cancers stained for human FAP (8). This similarity suggests that the HT-29 animal model of colorectal carcinoma will be useful in predicting clinically relevant tumor-stromal interactions. The HEK-FAP xenografts may be useful in assessing tumor biology in cancers characterized by FAP expression by tumor cells, as may be seen in some sarcomas (22). The studies described here establish a potentially pivotal role for FAP in the promotion of tumor growth, suggest avenues by which FAP function can be modulated, and describe murine systems for the analysis of FAP effects or functional inhibition of this protein.

ACKNOWLEDGMENTS

We thank the Hybridoma Facility and Pamela Nakajima for the hybridoma fusions and cell culturing and Research Pathology and Catherine Renner for the immunohistochemical staining.

REFERENCES

1. Niedermeyer, J., Scanlan, M. J., Garin-Chesa, P., Daiber, C., Fiebig, H. H., Old, L. J., Rettig, W. J., and Schnapp, A. Mouse fibroblast activation protein: molecular cloning, alternative splicing and expression in the reactive stroma of epithelial cancers. Int. J. Cancer, *71:* 383–389, 1997.
2. Scanlan, M. J., Raj, B. K., Calvo, B., Garin-Chesa, P., Sanz-Moncasi, M. P., Healey, J. H., Old, L. J., and Rettig, W. J. Molecular cloning of fibroblast activation protein α, a member of the serine protease family selectively expressed in stromal fibroblasts of epithelial cancers. Proc. Natl. Acad. Sci. USA, *91:* 5657–5661, 1994.
3. Niedermeyer, J., Enenkel, B., Park, J. E., Lenter, M., Rettig, W. J., Damm, K., and Schnapp, A. Mouse fibroblast-activation protein: conserved Fap gene organization and biochemical function as a serine protease. Eur. J. Biochem., *254:* 650–654, 1998.
4. Park, J. E., Lenter, M. C., Zimmermann, R. N., Garin-Chesa, P., Old, L. J., and Rettig, W. J. Fibroblast activation protein, a dual specificity serine protease expressed in reactive human tumor stromal fibroblasts. J. Biol. Chem., *274:* 36505–36512, 1999.
5. Garin-Chesa, P., Old, L. J., and Rettig, W. J. Cell surface glycoprotein of reactive stromal fibroblasts as a potential antibody target in human epithelial cancers. Proc. Natl. Acad. Sci. USA, *87:* 7235–7239, 1990.
6. Szeltner, Z., Renner, V., and Polgar, L. Substrate- and pH-dependent contribution of oxyanion binding site to the catalysis of prolyl oligopeptidase, a paradigm of the serine oligopeptidase family. Protein Sci., *9:* 353–360, 2000.
7. Altschul, S. F., Madden, T. L., Schaffer, A. A., Zhang, J., Zhang, Z., Miller, W., and Lipman, D. J. Gapped BLAST and PSI-BLAST: a new generation of protein database search programs. Nucleic Acids Res., *25:* 3389–3402, 1997.

8. Welt, S., Divgi, C. R., Scott, A. M., Garin-Chesa, P., Finn, R. D., Graham, M., Carswell, E. A., Cohen, A., Larson, S. M., Old, L. J., and Rettig, W. J. Antibody targeting in metastatic colon cancer: a Phase I study of monoclonal antibody F19 against a cell-surface protein of reactive tumor stromal fibroblasts. J. Clin. Oncol., *12:* 1193–1203, 1994.
9. Van den Hooff, A. Stromal involvement in malignant growth. Adv. Cancer Res., *50:* 159–196, 1988.
10. Adams, E. F., Newton, C. J., Braunsberg, H., Shaikh, N., Ghilchik, M., and James, V. H. Effects of human breast fibroblasts on growth and 17β-estradiol dehydrogenase activity of MCF-7 cells in culture. Breast Cancer Res. Treat., *11:* 165–172, 1988.
11. Camps, J. L., Chang, S. M., Hsu, T. C., Freeman, M. R., Hong, S. J., Zhau, H. E., von Eschenbach, A. C., and Chung, L.W. Fibroblast-mediated acceleration of human epithelial tumor growth *in vivo*. Proc. Natl. Acad. Sci. USA, *87:* 75–79, 1990.
12. Horgan, K., Jones, D. L., and Mansel, R. E. Mitogenicity of human fibroblasts *in vivo* for human breast cancer cells. Br. J. Surg., *74:* 227–229, 1987.
13. Duffy, M. J. Proteases as prognostic markers in cancer. Clin. Cancer Res., *2:* 613–618, 1996.
14. Stamenkovic, I. Matrix metalloproteinases in tumor invasion and metastasis. Semin. Cancer Biol., *10:* 415–433, 2000.
15. Stetler-Stevenson, W. G., and Yu, A. E. Proteases in invasion: matrix metalloproteinases. Semin. Cancer Biol., *11:* 143–153, 2001.
16. Johnson, J. P. Cell adhesion molecules in the development and progression of malignant melanoma. Cancer Metastasis Rev., *18:* 345–357, 1999.
17. Andreasen, P. A., Kjoller, L., Christensen, L., and Duffy, M. J. The urokinase-type plasminogen activator system in cancer metastasis: a review. Int. J. Cancer, *72:* 1–22, 1997.
18. Iwata, S., and Morimoto, C. CD26/dipeptidyl peptidase IV in context. The different roles of a multifunctional ectoenzyme in malignant transformation. J. Exp. Med., *190:* 301–305, 1999.
19. Graham, F. L., Smiley, J., Russell, W. C., and Nairn, R. Characteristics of a human cell line transformed by DNA from human adenovirus type 5. J. Gen. Virol., *36:* 59–74, 1977.
20. Cheng, H. C., Abdel-Ghany, M., Elble, R. C., and Pauli, B. U. Lung endothelial dipeptidyl peptidase IV promotes adhesion and metastasis of rat breast cancer cells via tumor cell surface-associated fibronectin. J. Biol. Chem., *273:* 24207–24215, 1998.
21. Dvorak, H. F. Tumors: wounds that do not heal. Similarities between tumor stroma generation and wound healing. N. Engl. J. Med., *315:* 1650–1659, 1986.
22. Rettig, W. J., Garin-Chesa, P., Beresford, H. R., Oettgen, H. F., Melamed, M. R., and Old, L. J. Cell-surface glycoproteins of human sarcomas: differential expression in normal and malignant tissues and cultured cells. Proc. Natl. Acad. Sci. USA, *85:* 3110–3114, 1998.

Promotion of Tumor Growth by Murine Fibroblast Activation Protein, a Serine Protease, in an Animal Model

Jonathan D. Cheng, Roland L. Dunbrack, Jr., Matthildi Valianou, et al.

Cancer Res 2002;62:4767-4772.